PNTIPROTON INDUCED NUCLEPR EXCITPTION PND FISSION*

T. VON EGIDY

Technische Universität München, D-85748 Garching, Germany
and
Institute des Sciences Nucléaires, F-38026 Grenoble, France

Representing the PS203 collaboration at LEARN/CERN

[H. Daniel, T. von Egidy, F.J. Hartmann, P. Hofmann, J. Hoffmann
Y.S. Kim, W. Schmid (Technische Universität München)
D. Hilscher, D. Polster, H. Rossner (Hahn–Meitner–Institut, Berlin)
J. Jastrzebski, W. Kurcewicz, P. Lubinski, A. Grabowska, A. Stolarz
(Warsaw University), H. Machner, G. Riepe (Forschungszentrum, Jülich)
A.S. Iljinov, A.S. Botvina, Ye.S. Golubeva, M.V. Mebel
(Russian Academy of Sciences, Moscow)
H.S. Plendl (Florida State University, Tallahassee)
J. Eades, S. Neumaier (CERN, Geneva)]

(Received July 2, 1993)

The annihilation of stopped antiprotons at the nuclear surface produced 2–8 pions. Some of them enter the nucleus and can heat it up to nearly 1 GeV excitation energy. We measured with a new double-arm fission fragment spectrometer the masses and kinetic energies of both fragments and their folding angle. The number of particles emitted before and after scission was deduced. Absolute fission rates are determined for some targets. Particle spectra and the distribution of residual nuclei were measured. The neutron-to-proton density ratio in the periphery of nuclei was determined with a new neutron halo effect during the antiproton annihilation. Detailed intranuclear cascade calculations reproduce most of the experimental results.

PACS numbers: 25.43. +t, 25.85. -w

---

* Presented at the Meson–Nucleus Interactions Conference, Cracow, Poland, May 14–19, 1993.

1. Introduction

The antiproton is a very interesting probe to investigate nuclei under unusual conditions. Stopped antiprotons form antiprotonic atoms, cascade down by emission X-rays and annihilate with a nucleon at the nuclear surface. The annihilation energy of 1.88 GeV is transformed into the pions and some kaons (sometimes following intermediate mesons). Some mesons penetrate the nucleus and start an intranuclear cascade with fast proton and neutron emission and composite particle emission by coalescenece. The equilibration process results in a heated nucleus with excitation energies ranging up to nearly 1GeV. In contrast to heavy ion reactions this high excitation energy is achieved without large angular momentum transfer and without compression. The heated nucleus evaporates mainly neutrons and reaches the ground state which is frequently radioactive. In heavier nuclei fission competes with evaporation. However, it has to be kept in mind that there is also some chance that no pion interacts with the nucleus and that the nucleus is left with only one nucleon missing. The yield of these (A-1)-nuclei (A=mass number of the target) gives information on the neutron halo. A review on antiproton-nucleus interaction is found in Ref. [1].

Our group investigated at the Low Energy Antiproton Ring LEAR at CERN (PS 186 and PS 203) the principal processes after the annihilation of stopped antiprotons at target nuclei between Li and U, *i.e.*, particle spectra [2–5], distributions of residual nuclei [6–11], fission [10, 12–16] and the neutron halo effect [17]. In the present contribution we shall discuss some of our newest experimental results in these fields. Our experiments are compared with intranuclear cascade calculations using the Monte Carlo method. These calculations take into account the fast intranuclear cascade with particle emission (for composite particles by coalescence), pre-equilibrium processes which result in a thermalized hot nucleus, and finally evaporation of neutrons and of few other particles competing with fission for heavy nuclei.

2. Antiproton induced fission

A double-arm fission fragment spectrometer was constructed to measure kinetic energies, time-of-flight and folding angle of both coincident fragments after fission induced by antiprotons stopped in targets of U, Th and Bi [12]. The spectrometer consists of two PIN-diode arrays (each with 12×12 PIN-diodes, each diode with an area of 1 cm^2) at a distance of 60 cm at opposite sides of the target. This spectrometer yields distributions of kinetic energies and masses of individual fragments, distributions of total masses and total kinetic energies, the folding angle between two fragments, the momentum of the fissioning nucleus and various correlations between these

values [13, 16]. Fig. 1 shows for the U target the mass distribution of individual fission fragments and the total kinetic energy distribution and compares them with calculations. The good agreement between theory and experiment justifies the application of the intranuclear cascade and of the fission model for the study of energy dissipation and scission of hot nuclei after antiproton–nucleus annihilation.

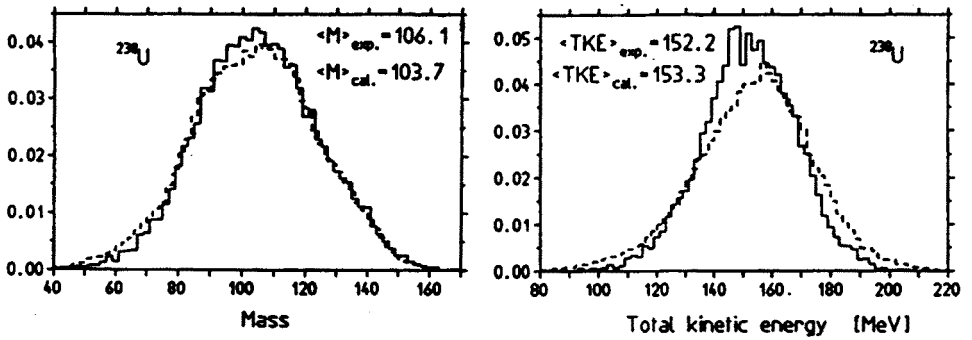

Fig. 1. Mass distribution of fission fragments (left) and total kinetic energy distribution (right) of antiproton induced fission. The experimental (solid histogram) and calculated (dashed histogram) distributions are normalized to one fission event.

The total mass loss is a measure for the excitation energy. Different mass loss windows show asymmetric fission for low excitation energy and symmetric fission for higher excitation energies. The momentum ratio of the heavier and lighter fragment is expected to be 1, if fission takes place after thermalization (see Chestnov *et al.* [18]). The increase of this ratio above a mass loss of 40 u (300–400 MeV excitation energy) in Fig. 2 indicates that there is also fission before thermalization.

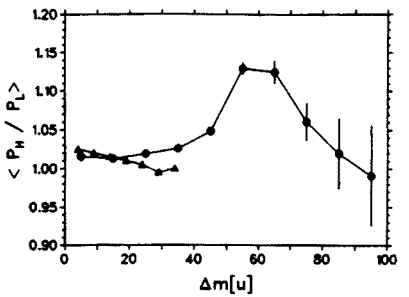

Fig. 2. Momentum ratio of heavy and light fission fragments of the U target as a function of the mass loss (circle: stopped antiprotons; triangle: 1 GeV p [18]).

A new method was developed to deduce the number of particles emitted before and after scission from the correlation between total kinetic energy

and total mass [19]. This evaluation gave for the U target the surprising result that up to 40 nucleons are emitted after scission for a mass loss of 60–70 u in contrast to heavy-ion reactions [20]. In order to investigate this discrepancy a new experiment was designed which applies kinematic focussing to distinguish neutrons emitted before and after scission. Neutrons after scission are preferentially emitted in the direction of the fission axis. The new apparatus is shown in Fig. 3 with six PIN-diode arrays (each 6×12 diodes) and four neutron counters which determine the neutron energy by time-of-flight. The first evaluation (Fig. 4) demonstrates that more neutrons are emitted with an angle of 0 degree to the fission axis than with 90 degree, but the difference is not as large as expected from the previous experiment.

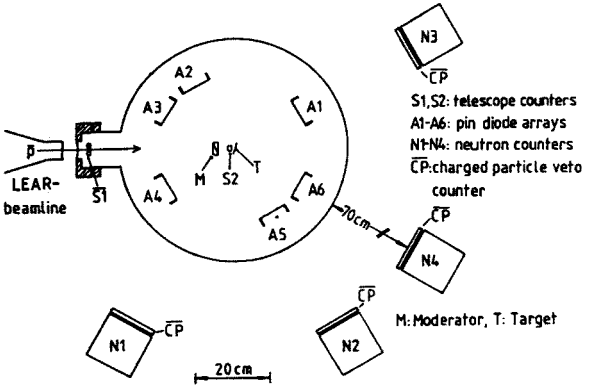

Fig. 3. Fragment spectrometer with particle detectors for antiproton induced fission.

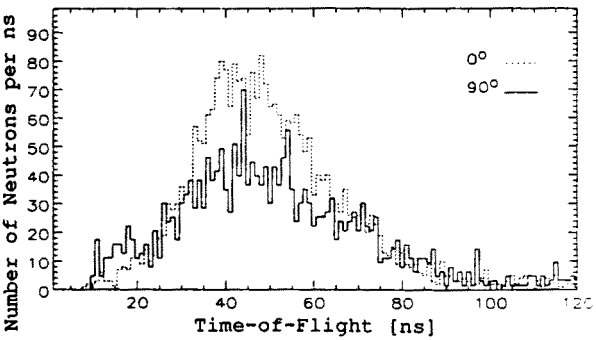

Fig. 4. Time-of-flight neutron spectrum emitted after antiproton induced fission in U at angles of 0 degree and 90 degree to the fission axis.

Absolute fission probabilities per stopped antiproton were obtained with a special arrangement using two PIN-diodes close to the target to identify

coincident fission fragments [15]. Table I compares the experimental results with new calculations. The experimental values for Ag and Cu are only roughly estimated upper limits.

TABLE I

Experimental and calculated absolute fission probabilities per stopped antiproton in %:

Target	Experiment	Calculation
U	77.0(4)	81.3
Th	70.0(4)	72.5
Au	3.1(3)	5.42
Ho	< 1.1	0.58
Ag	(< 0.4)	0.25
Cu	(< 1.9)	1.59

The calculations are described in [15] and use the modified liquid drop model [21].

3. Particle emission

In our previous experiments [2–4] we measured p, d, t, ^{3}He and ^{4}He spectra with Ge and Si telescopes with targets between Li and U. One of the results was that all spectra have exponential shapes above 25 MeV. The distribution of the momentum square p^2 of the ejectiles can be described in all cases by $\exp(p^2/q^2)$ where q seems to be a universal constant for nearly all targets and ejectiles on averages with $q = 360$ MeV/c.

New experiments to measure inclusive particle spectra were performed with scintillation detectors (NE 213, 12.5 cm diameter $\times$10 cm) and time-of-flight techniques [5]. K, π, n, p, d and t spectra were obtained for a series of targets. The multiplicity of charged K's in the range 64 to 180 MeV for the U target was found to be 0.043(13) with a very small energy slope. Neutron and proton spectra for Cu and U targets are shown in Fig. 5. In the case of U three sources may be associated with different stages in the antiproton–nucleus interaction. The fast stage of the internuclear cascade is dominated by sequential two-body collisions of the annihilation pions with nucleons and leads to high energy particles (dashed fraction of the spectra). The

intermediate component corresponds to pre-equilibrium emission (dotted line for n in U). During the third stage neutrons are evaporated from the compound system and from fission fragments (dashed–doted line for n). No second component was observed for the Cu target, because less energy is deposited in this nucleus and the multiplicity of pre-equilibrium neutrons is low. The ratio of directly emitted neutrons and protons is 3.0(6) for Cu and 3.2(5) for U. The calculations predict lower ratios and different ones for Cu and U. These ratios are sensitive tests to isospin effects and represent a considerable challenge to intranuclear cascade models.

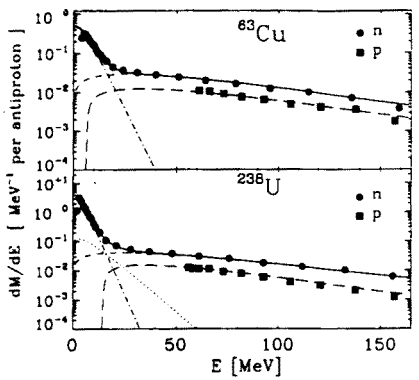

Fig. 5. Energy spectra of neutrons and protons after antiproton annihilation in Cu and U. The curves are explained in the text and in [5].

4. Residual nuclei

The distribution of residual nuclei after antiproton annihilation corresponds to the mass loss which is a measure of the excitation energy of the hot compound nucleus before evaporation and fission. These distributions for several target nuclides were determined by measuring the gamma spectra of the irradiated targets [6–11]. The general features of these distributions are similar to the distributions after nuclear reactions with relativistic ions [9]. This is demonstrated in Fig. 6 where the distribution after stopped antiproton annihilation in Au is compared with the distribution of 1GeV p reactions with Au [22]. Intranuclear cascade calculation can reproduce even details of the distributions and allow to test special reaction mechanisms. For instance the trawling effect, the reduction of nuclear density behind fast moving particles, seems to play no role in our case.

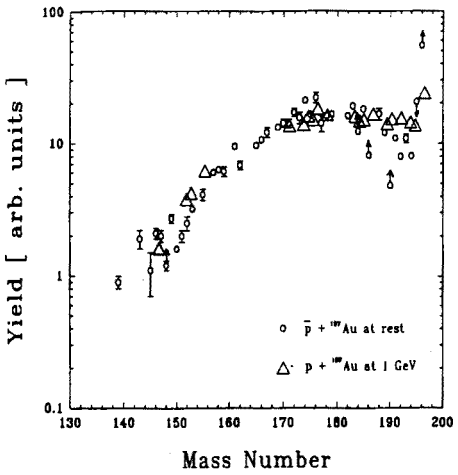

Fig. 6. Comparison of the mass yield distributions of antiproton and 1 GeV p [22] induced reactions with Au.

5. The neutron halo effect after antiproton annihilation

After the annihilation of stopped antiprotons not only very hot nuclei are produced, but also some cold nuclei with only one nucleon missing due to the annihilation. In these cases, mainly annihilations in the far periphery of the nucleus, the pions do neither transfer much energy to the nucleus nor eject particles. From a target nucleus with Z protons and N neutrons the nuclides $(Z-1, N)$ and $(Z, N-1)$ are formed by annihilation at a proton or neutron, respectively. The ratio of the yield of these $(A-1)$ nuclides is a measure for the neutron-to-proton density ratio in the nuclear periphery. First results were obtained with a Th target [17]. The following yields Y were obtained for $(N-1)$ and $(Z-1)$ nuclides and a neutron halo factor f was deduced:

^{231}Th: $Y(N-1) = 10.0(27)$ per 100 annihilations;
^{231}Ac: $Y(Z-1) = 1.29(16)$ per 100 annihilations;
Annihilation ratio: $Y(N-1)/Y(Z-1) = 7.8(22)$;
Halo factor: $f = (Y(N-1)/Y(Z-1))(Z/N)a = 7.8(22)$.

The parameter $a = 1.59$ is the ratio of the antiproton absorption probabilities at a proton to the one at a neutron [23]. Our most recent results show that the halo factor is nearly 1 for nuclides with a closed neutron shell and that it increases with decreasing neutron binding energy. Calculations to interpret this neutron halo effect have started.

6. Summary

Our experimental results show that a wealth of very interesting information on very hot and also on cold nuclei can be obtained by stopped antiproton annihilation. Asymmetric, symmetric and pre-equilibrium fission was observed. Absolute fission probabilities were determined. Intranuclear cascade calculations and a newly developed high-energy fission model reproduce various fission distributions quite well. In order to determine the time scale of fission, the number of particles emitted before and after scission was deduced from the total kinetic energy, total mass correlation and more recently from neutron spectra measurements in coincidence with fission fragments.

An unexpected result which is not yet explained by theoretical calculations, is the ratio of fast neutrons to fast protons being about 3 for Cu and U as well. Probably new reaction mechanisms have to be invoked to understand this ratio.

Residual nuclei distributions and their interpretation show the similarity of antiproton and relativistic ion reactions. However, reactions with fast antiprotons might be different, because more energy can be transferred to the nucleus at small angular momentum.

The new neutron halo effect needs further experimental and theoretical systematic investigations in order to extract from the experimental neutron-to-proton annihilation ratio, the density ratio and the radius where it is measured.

Further experiments on antiproton-nucleus interaction will concentrate on nuclear excitation, fission and multifragmentation induced by stopped and by fast antiprotons in order to obtain detailed information on hot nuclear matter with low spin and without compression.

The work was supported by the German Bundesministerium für Forschung und Technologie, by the Deutsche Forschungsgemeinschaft, by the Polish State Committee for Scientific Research and by the Polish–German Collaboration Agreement.

REFERENCES

[1] T. von Egidy, *Nature* **328**, 773 (1987).

[2] W. Markiel, H. Daniel, T. von Egidy, F.J. Hartmann, P. Hofmann, W. Kanert, H.S. Plendl, K. Ziock, R. Marschall, H. Machner, G. Riepe, J.J. Reidy, *Nucl. Phys.* **A485**, 445 (1988).

[3] P. Hofmann, F.J. Hartmann, H. Daniel, T. von Egidy, W. Kanert, W. Markiel, H.S. Plendl, H. Machner, G. Riepe, D. Protic, K. Ziock, R. Marshall, J.J. Reidy, *Nucl. Phys.* **A512**, 669 (1990).

[4] A.S. Sudov, A.S. Botvina, A.S. Iljinov, Ye. S. Golubeva, V.G. Nedorezov, H. Daniel, T. von Egidy, F.J. Hartmann, P. Hofmann, W. Kanert, H.S. Plendl, G. Schmidt, C.A. Schug, G. Riepe, *Nucl. Phys.* **A554**, 223 (1993).

[5] D. Polster, D. Hilscher, H. Rossner, W. Schmid, P. Baumann, H. Daniel, T. von Egidy, F.J. Hartmann, P. Hofmann, Y.S. Kim, M.S. Lotfranaei, *Phys. Lett.* **B300**, 317 (1993).

[6] E.F. Moser, H. Daniel, T. von Egidy, F.J. Hartmann, W. Kanert, G. Schmidt, M. Nicholas, J.J. Reidy, *Phys. Lett.* **B179**, 25 (1986).

[7] E.F. Moser, H. Daniel, T. von Egidy, F.J. Hartmann, W. Kanert, G. Schmidt, Ye.S. Golubeva, A.S. Iljinov, M. Nicholas, J.J. Reidy, *Z. Phys.*, **A333**, 89 (1989).

[8] T. von Egidy, H. Daniel, F.J. Hartmann, W. Kanert, E.F. Moser, Ye.S. Golubeva, A.S. Iljinov, J.J. Reidy, *Z. Phys.* **A335**, 451 (1990).

[9] T. von Egidy, H.H. Schmidt, *Z. Phys.* **A341**, 79 (1991).

[10] H, Machner, Sa Jun, G. Riepe, D. Protic, H. Daniel, T. von Egidy, F.J. Hartmann, W. Kanert, W. Markiel, H.S. Plendl, K. Ziock, R. Marshall, J.J. Reidy, *Z. Phys.* **A343**, 73 (1992).

[11] J. Jastrzębski, W. Kurcewicz, P. Lubiński, A. Grabowska, A. Stolarz, H. Daniel, T. von Egidy, F.J. Hartmann, P. Hofmann, Y.S. Kim, A.S. Botvina, Ye.S. Golubeva, A.S. Iljinov, G. Riepe, H.S. Plendl, *Phys. Rev.* **C47**, 216 (1993).

[12] Y.S. Kim, P. Hofmann, H. Daniel, T. von Egidy, T. Haninger, F.J. Hartmann, M.S. Lotfranaei, H. Plendl, *Nucl. Instrum. Methods* **A329**, 403 (1993).

[13] P. Hofmann, Y.S. Kim, H. Daniel, T. von Egidy, T. Haninger, F.J. Hartmann, P. David, H. Machner, G. Riepe, H.S. Plendl, K. Ziock, B. Wright, D. Bowman, W. Lynch, J. Lieb, J. Jastrzębski, W. Kurcewicz, *Sov. J. Nucl. Phys.* **55**, 713 (1992).

[14] T. von. Egidy, H. Daniel, F.J. Hartmann, P. Hofmann, Y.S. Kim, W. Schmid, H.H. Schmidt, G. Riepe, H. Machner, P. David, H.S. Plendl, A.S. Iljinov, A.S. Botvina, Ye.S. Golubeva, M.V. Mebel, J. Jastrzębski, W. Kurcewicz, *Nucl. Phys.* **558**, 383c (1993).

[15] W. Schmid, P. Baumann, H. Daniel, T. von. Egidy, F.J. Hartmann, P. Hofmann, Y.S. Kim, H.H. Schmidt, A.S. Iljinov, M.V. Mebel, D. Hilscher, D. Polster, H. Rossner,*Nucl. Phys. A* , accepted for publication.

[16] P. Hofmann, A.S. Iljinov, Y.S. Kim, M.V. Mebel, H. Daniel, P. David, T. von Egidy, T. Haninger, F.J. Hartmann, J. Jastrzębski, W. Kurcewicz, J. Lieb, H. Machner, H.S. Plendl, G. Riepe, B. Wright, K. Ziock, *Phys. Rev C.*, to be submitted.

[17] J. Jastrzębski, H. Daniel, T. von Egidy, A. Grabowska, Y.S. Kim, W. Kurcewicz, P. Lubiński, G. Riepe, W. Schmid, A. Stolarz, S. Wycech, *Nucl. Phys.* **558**, 405c (1993).

[18] Yu. A. Chestov, A.V. Kravtsov, B.Yu. Sokolovskii, G.E. Solyakin, *Sov. J. Nucl. Phys.* **45**, 11 (1987).

[19] Y.S. Kim, PhD Thesis, Technical University Munich, 1992.

[20] D.J. Hinde, D. Hilscher, H. Rossner, *Nucl. Phys.* **A502**, 497c (1989).

[21] H.J. Krappe, J.R. Nix, A.S. Sierk, *Phys. Rev.* **C20**, 992 (1979).
[22] S.B. Kaufman, E.P. Steinberg, *Phys. Rev.* **C22**, 167 (1980).
[23] W.M. Bugg *et al.*, *Phys. Rev. Lett.* **31**, 475 (1973).